

The History of Inflation from Microwave Background Polarimetry and Laser Interferometry

Jerod Caligiuri and Arthur Kosowsky

Department of Physics and Astronomy, University of Pittsburgh, Pittsburgh, PA 15260 USA and Pittsburgh Particle Physics, Astrophysics, and Cosmology Center (PITT PACC), Pittsburgh, PA 15260 USA

William H. Kinney

Department of Physics, University at Buffalo, Buffalo, NY 14260 USA

Naoki Seto

Department of Physics and Astronomy, Kyoto University, Kyoto 606-8502 JAPAN

(Dated: September 5, 2014)

A period of inflation in the early universe produces a nearly scale-invariant spectrum of gravitational waves over a huge range in wavelength. If the amplitude of this gravitational wave background is large enough to be detectable with microwave background polarization measurements, it will also be detectable directly with a space-based laser interferometer. Using a Monte Carlo sampling of inflation models, we demonstrate that the combination of these two measurements will strongly constrain the expansion history during inflation and the physical mechanism driving it.

PACS numbers: 04.80.Nn, 98.70.Vc, 98.80.Cq, 98.80.Es

Introduction. The recent detection of B-mode microwave background polarization [1, 2] at large angular scales by the BICEP2 experiment [3] may arise from a stochastic background of gravitational waves generated during inflation in the early universe. Polarized emission from galactic dust is also a possible source of this signal [4, 5], but if a significant fraction of the signal is in fact of primordial origin, it provides an otherwise unobtainable window into physics at extremely high energies.

A period of exponential expansion in the early universe, known as inflation, resolves several observational difficulties with the standard cosmological model (e.g., [6–15]). Such a period of expansion can be driven by some component with a nearly constant energy density, such as the potential energy of an effective scalar field (the “inflaton”). During this epoch, quantum fluctuations in the inflaton field are amplified into classical density perturbations which grow by gravitational instability into the structures visible in the universe today. Likewise, quantum fluctuations in the tensor components of the inflating spacetime are amplified into a stochastic background of gravitational waves, with a nearly scale-invariant power spectrum and an amplitude depending on the energy scale of inflation. Once generated, these tensor perturbations propagate almost freely through the universe, their wavelengths increased by the expansion of the universe and their amplitudes decreased by the same factor once the wavelength comes inside the horizon.

The hallmark of an inflationary gravitational wave background is its extremely wide range in wavelengths, roughly from the scale of the horizon today down to terrestrial scales. If inflation occurred when the temperature of the universe was around the Grand Unification scale of 2×10^{16} GeV, the gravitational wave background

will make a pattern of B-mode polarization large enough to be seen in the current BICEP2 data. Remarkably, an inflationary tensor perturbation signal of this amplitude will likely also be detectable directly with future space-based laser interferometers [16–25]. Direct detection will probe wavelengths that are 15 orders of magnitude smaller than those inducing microwave background signals; measurements at these two scales probe a large portion of the observable inflation epoch, and may therefore reveal the physical process driving inflation.

A recent paper showed that an interferometric detection of the inflationary tensor signal will provide qualitatively new information about inflation, namely a precise measurement of any departure from a pure power-law spectrum [26]. If we can obtain information about inflation at widely varying scales, a natural question arises: ultimately, how well can the history of inflation, and the physics driving it, be determined? Here, we determine constraints on the effective potential governing the evolution of the inflaton from future measurements from both microwave background and local scales. We use a Monte Carlo method to generate random inflation models with slowly varying inflaton value (the so-called “slow roll” condition) at the time when perturbations on the scale of the horizon today are generated [27, 28] and which satisfy current measurements, including the nominal BICEP2 range for the tensor amplitude. Of these models, only a very small fraction satisfy tensor amplitude constraints at the few percent level on both scales, and the resulting effective inflaton potentials are all very similar. Other recent work uses similar techniques to constrain inflation using only microwave background measurements [29]; our results show that the additional information from an interferometric detection greatly restricts the range of ac-

ceptable inflation models.

Methods. We compute the dynamical history and resulting scalar and tensor perturbation spectra for random inflation models chosen via the technique of Monte Carlo inflation flow potential reconstruction [27, 28]. The dynamics of an inflation model can be written in terms of the value of an effective scalar field ϕ (the “inflaton”) and its potential energy $V(\phi)$; inflation occurs when the energy density is dominated by the inflaton potential energy. The field ϕ will evolve towards the minimum of the potential as inflation progresses. It is convenient to use the value of the effective inflaton field ϕ during inflation as a time parameter; this can be done as long as ϕ evolves monotonically to smaller values. The Hubble parameter during inflation, $H \equiv (1/a)da/dt$ with $a(t)$ the scale factor, can be used to construct a hierarchy of “slow-roll parameters” [30]

$$\begin{aligned}\epsilon &\equiv \frac{m_{\text{Pl}}^2}{4\pi} \left(\frac{H'(\phi)}{H(\phi)} \right)^2, \\ \sigma &\equiv \frac{m_{\text{Pl}}}{\pi} \left[\frac{1}{2} \left(\frac{H''}{H} \right) - \left(\frac{H'}{H} \right)^2 \right], \\ {}^\ell \lambda_{\text{H}} &\equiv \left(\frac{m_{\text{Pl}}^2}{4\pi} \right)^\ell \frac{(H')^{\ell-1} d^{(\ell+1)}H}{H^\ell d\phi^{(\ell+1)}}, \quad \ell \geq 2.\end{aligned}\quad (1)$$

where primes are derivatives with respect to ϕ and the Planck mass m_{Pl} sets the energy units. The evolution of the parameters during inflation is determined by a system of first-order linear equations [27, 31],

$$\begin{aligned}\frac{d\epsilon}{dN} &= \epsilon(\sigma + 2\epsilon), \\ \frac{d\sigma}{dN} &= -5\epsilon\sigma - 12\epsilon^2 + 2({}^2\lambda_{\text{H}}), \\ \frac{d({}^\ell\lambda_{\text{H}})}{dN} &= \left[\frac{\ell-1}{2}\sigma + (\ell-2)\epsilon \right] ({}^\ell\lambda_{\text{H}}) + {}^{\ell+1}\lambda_{\text{H}}.\end{aligned}\quad (2)$$

In these equations the time variable is the number of expansion e-folds before the end of inflation $N \equiv \ln(a_{\text{end}}/a)$ where

$$\frac{d}{dN} = \frac{m_{\text{Pl}}}{2\pi^{1/2}} \sqrt{\epsilon} \frac{d}{d\phi}.\quad (3)$$

Given a solution for $\epsilon(\phi)$, $H(\phi)$ can be obtained from the definition of ϵ , and the effective potential $V(\phi)$ then follows from the equation of motion for $H(\phi)$,

$$H^2(\phi) \left[1 - \frac{1}{3}\epsilon(\phi) \right] = \frac{8\pi}{3m_{\text{Pl}}^2} V(\phi).\quad (4)$$

A particular model of inflation is obtained by choosing initial values for the slow-roll parameters; its dynamical evolution corresponds to some trajectory in the slow-roll parameter space. In practice, we truncate the hierarchy Eqs. (2) above $\ell = 8$ (corresponding to a restricted subset of exact inflation models) and then evolve the evolution equations until inflation ends, which we take as

the condition $\epsilon = 1$. Once the slow-roll parameters are all determined throughout inflation as a function of N , the fractional density perturbation $\delta\rho/\rho$ arising from the scalar perturbations and the tensor/scalar ratio r are, to second-order in the slow roll parameters, given by [30, 32],

$$\begin{aligned}\frac{\delta\rho}{\rho} &\simeq \frac{H}{2\pi m_{\text{Pl}} \sqrt{\epsilon}}, \\ r &\simeq 16\epsilon [1 - C(\sigma + 2\epsilon)]\end{aligned}\quad (5)$$

with $C \equiv 4(\ln 2 + \gamma) - 5 = 0.0814514$, where $\gamma \simeq 0.577$ is Euler’s constant, and using the WMAP normalization convention for r [33]. Then the perturbation amplitudes as a function of N can be converted to amplitudes as a function of comoving wavenumber k at the end of inflation by the relation $a(N)H(N) = k$. Generating scalar and tensor perturbations for a random sampling of inflation models is thus reduced to choosing random initial points in the slow-roll parameter space. The resulting primordial scalar perturbation power spectrum $P(k) \simeq A_S(k/k_0)^{n_S-1}$ and tensor power spectrum $P_T(k) \simeq A_T(k/k_0)^{n_T}$ are both approximate power laws on cosmological scales around $k_0 = 0.002 \text{ Mpc}^{-1}$, with $r \equiv A_T/A_S$.

We initially select models within an ellipsoidal parameter space region with principal axes $0.952 < n_S < 0.981$, $0.078 < r < 0.265$, and $-0.001 < dn_S/d\ln k < 0.001$; these ranges are consistent with the 95% confidence region from current Planck [34], WMAP polarization [35], and BICEP2 microwave background measurements [3] (assuming the BICEP2 signal is due to tensor perturbations) and baryon acoustic oscillation measurements from the Sloan Digital Sky Survey Data Release 9 [36], the 6dF Galaxy Survey [37], and the WiggleZ Dark Energy Survey [38] (shown in Fig. 5 of Ref. [39]). The full tensor spectrum is then computed by exact numerical evaluation of the mode equation for the cosmological background defined by the selected solution to the flow equations, in place of the slow-roll approximation in Eq. (5). The corresponding inflation potential $V(\phi)$ is also computed numerically for each model.

Given the tensor perturbation spectrum from a particular inflation model, we obtain the tensor spectrum in the present universe using well-known techniques for computing the transfer function for the amplitudes and wavelengths [19, 40–42], assuming the standard Λ CDM cosmology [34]. For simplicity, we assume that the reheating phase after inflation, in which the energy density stored in the kinetic energy of the inflaton field is converted to a thermal bath of relativistic particles, occurs rapidly on a time scale short compared to the Hubble time. We then compute a signal for both B-mode polarization and laser interferometry from the tensor perturbations in each model.

The detected BICEP B-mode polarization signal corresponds to a tensor amplitude $r = 0.16$ with a 95%

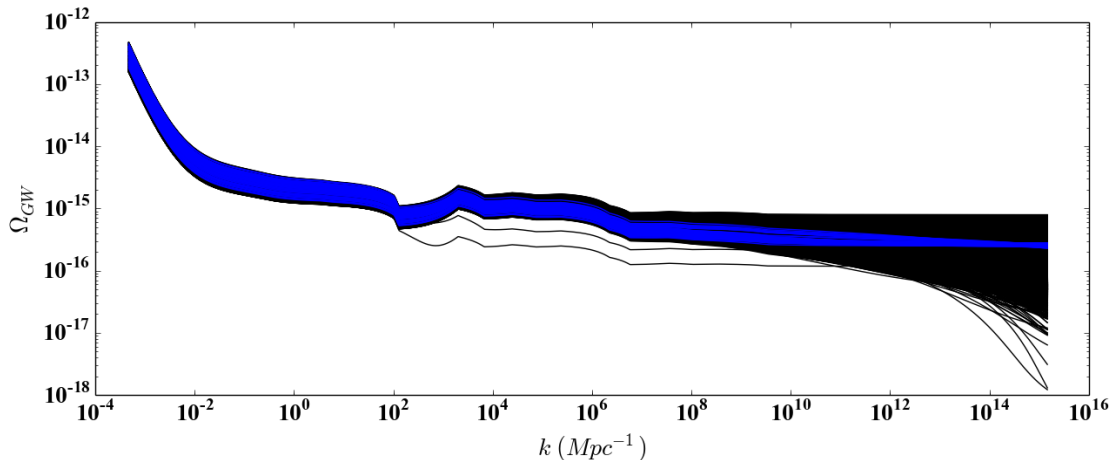


FIG. 1: Inflationary tensor perturbation spectra $\Omega_{\text{GW}}(k)$ today per unit logarithmic frequency interval, in units of critical density, assuming evolution of the universe in the standard cosmological model and instantaneous reheating after inflation. These spectra are obtained from Monte Carlo initial conditions for Eqs. (2), truncated after $\ell = 8$. Black curves display 2×10^4 models consistent at 2σ with microwave background measurements from Planck, baryon acoustic oscillation measurements, and BICEP2, assuming the BICEP2 signal is due to tensor perturbations. The 66 models in blue are also consistent with a hypothetical direct amplitude measurement from a space-based interferometer with a fiducial amplitude of $\Omega_{\text{GW}} = (2.6 \pm 0.2) \times 10^{-16}$ at a frequency of $f = 0.25$ Hz, corresponding to a wavenumber of $k = 1.6 \times 10^{14} \text{ Mpc}^{-1} = 5.2 \times 10^{-6} \text{ km}^{-1}$.

The scale of the horizontal axis assumes a Hubble parameter $h = 0.68$.

confidence level range roughly from 0.10 to 0.30. For interferometers, a stochastic gravitational wave power spectrum is often expressed as $\Omega_{\text{GW}}(f)$, the fraction of critical density in gravitational waves per unit logarithmic frequency interval. We assume a particular fiducial model of the local tensor perturbations with an amplitude of $\Omega_{\text{GW}} = 2.6 \times 10^{-16}$ at a frequency of $f = 0.25$ Hz. We then consider a measurement of this amplitude with a 2σ standard error of around 7%: this corresponds to the reference strain sensitivity $u\sqrt{S_{\text{base}}(f)}$ of the DECIGO effective interferometer design given in Fig. 2 of [43], with $u = 1/3$ and a low-frequency cutoff of 0.2 Hz to minimize the contaminating astrophysical foreground signal from white dwarf binaries. We also assume perfect removal of neutron star and black hole binary signals. (One interferometer design attaining these specifications comprises four sets of three detectors with optimal sensitivity around 1 Hz. Each group can effectively generate two independent interferometers by taking appropriate combinations of data streams from the set. Pairs of these groups will have overlapping orbits to facilitate correlation analysis. Such an experiment is clearly ambitious, but achievable with known technology at a cost comparable to current large physics and astronomy efforts.) A particular inflation model is considered consistent with the fiducial interferometer signal if its amplitude is within the 2σ range for Ω_{GW} over the frequency band from 0.2 to 20 Hz.

Results. Figure 1 displays the tensor perturbation spectra today for 2×10^4 random inflation models satisfy-

ing the joint Planck and BICEP2 constraints (assuming the entire BICEP2 B-mode signal is due to tensor perturbations) on the scalar perturbation amplitude, scalar spectral index, and tensor-scalar ratio. The spectrum features are due to the evolution of the relativistic degrees of freedom after inflation. Of these 2×10^4 models, only 66 (blue curves in Fig. 1) are also consistent with our fiducial interferometer constraint on the local tensor amplitude. The measurement of the local tensor amplitude by an interferometer reduces the number of allowed slow-roll inflation models by a factor of 300.

Figure 2 shows the effective inflaton potentials for the models in Fig. 1. Here we plot in different colors the models consistent both with the interferometer constraint, and also with various values of the tensor/scalar ratio r from B-mode polarization: from top to bottom, the bands correspond to $r = 0.18$, $r = 0.16$, $r = 0.14$, and $r = 0.10$, each with a range of ± 0.005 . The portions of the colored potentials above the dashed line correspond to the perturbations between the B-mode polarization scale and the interferometer scale. Each band of potentials all look very similar to each other across the range of wavelengths probed. In essence, this combination of measurements constrains the model of inflation with little uncertainty, given our assumption of instantaneous reheating.

This conclusion will hold even for tensor spectra with a significantly lower amplitude than the BICEP2 measurement, provided that the amplitude can still be measured on both scales with similar fractional errors as used here.

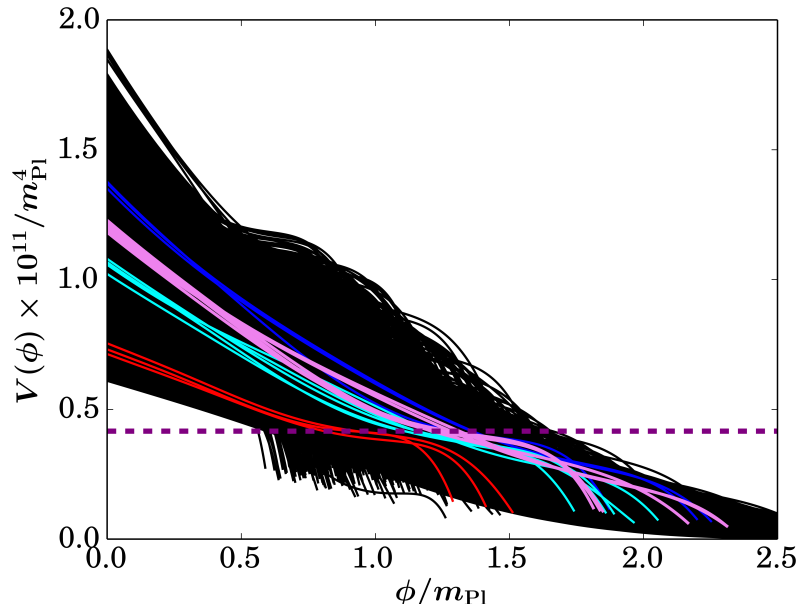


FIG. 2: Effective inflaton potentials $V(\phi)$ corresponding to the 2×10^4 models in Fig. 1. The potentials are aligned so that 60 e-foldings before the end of inflation, around when tensor perturbations visible in B-mode microwave background polarization were generated, is at the left edge of the plot. The bands of colored potentials contain those which satisfy both the hypothetical 7% direct amplitude measurement from a space-based interferometer shown by the blue curves in Fig. 1, and also a constraint on r of ± 0.005 . The colored bands have, from top to bottom, central values of $r = 0.18$ (3 models), $r = 0.16$ (6 models), $r = 0.14$ (5 models), and $r = 0.10$ (3 models). The dashed line intersects the colored potentials at around 20 e-foldings before the end of inflation, where tensor perturbations detectable by interferometry were generated.

Of course, the lower the amplitude, the more technically challenging these measurements become. For amplitudes significantly below $r = 10^{-3}$, confusion with the residual gravitational lensing signal will prevent measurement of the tensor amplitude using B-mode polarization [44, 45], while the binary confusion limit becomes an increasing problem for interferometer measurements.

Discussion. These results clearly demonstrate the über-coolness of combined measurements of the tensor power spectrum amplitude at both microwave background and interferometric scales. The family of inflation models consistent with both measurements is vastly restricted compared to inflation models consistent only with an amplitude measurement at a single scale. Furthermore, the combined measurements determine the inflaton potential over a wide range of field values. We have assumed B-mode polarization measurements of the tensor amplitude with precision at the $r = 0.005$ level; upcoming polarization experiments with increased sensitivity and frequency coverage are expected to surpass this (see, e.g., [46]). We also assume a future interferometer measurement of the tensor amplitude at the 7% level, which will be challenging but feasible if the BICEP2 signal has a non-negligible tensor contribution.

We have made the simplifying physical assumption that reheating after inflation happens quickly, meaning

on a time scale less than a Hubble time so it has little effect on the expansion history of the universe. Some models of reheating take significantly longer than this, resulting in a period of matter-dominated expansion prior to the usual radiation-dominated era which can modify the tensor amplitude at small scales (e.g., [47]). Measurements of both the tensor amplitude and the scalar spectral index will give interesting constraints on the duration of any reheating epoch [48]. An extension of the present analysis to include reheating will be considered elsewhere.

The numerical analysis in this paper does not have a rigorous quantification of Monte Carlo coverage of the inflation model space. The truncation of the slow-roll hierarchy at a given order results in only a particular subset of inflation models in the allowed model space. Larger computational efforts can include higher-order truncations, effectively expanding the model space which is explored, and more total models in each Monte Carlo, which will sharpen statistical conclusions. It is unlikely that models not available in our 8th-order slow-roll hierarchy will change our conclusions in a qualitative sense, since the allowed models span a wide range of potentials, as is visible in Fig. 2. However, whether rare successful models exist which are clearly different from the family of models identified here is an interesting open question.

These rare cases may be further constrained by additional sources of information. For example, we have not included any constraints on the tensor power spectrum aside from amplitude; full-sky, high resolution microwave polarization maps may deliver restrictive measurements of the tensor spectral index n_T at cosmological scales [26, 49].

The results presented here show that a detection of inflationary tensor perturbations at two widely separated scales, the cosmological scale via B-polarization of the microwave background and the Earth-Moon scale via a space-based laser interferometer, will determine the dynamical history of the universe during the inflation era. In turn, such measurements will give strong constraints on fundamental physics at energy scales of 10^{16} GeV, inaccessible by any other means.

A.K. thanks B. Fishbain for helpful suggestions. J.C. and A.K. are supported in part by the National Science Foundation under grant NSF-AST-1312380. W.H.K. is supported by the National Science Foundation under grants NSF-PHY-1066278 and NSF-PHY-1417317. N.S. is supported by MEXT grant 24103006. Computations were performed in part at the University at Buffalo Center for Computational Research. Flowcode 1.0.3, used to perform the inflation flow Monte Carlo, was written by Brian A. Powell and W.H.K. This work has used NASA's Astrophysical Data System for bibliographic information.

-
- [1] M. Kamionkowski, A. Kosowsky, and A. Stebbins, *Phys.Rev.* **D55**, 7368 (1997), astro-ph/9611125.
- [2] M. Zaldarriaga and U. Seljak, *Phys.Rev.* **D55**, 1830 (1997), astro-ph/9609170.
- [3] P. Ade et al. (BICEP2 Collaboration), *Phys.Rev.Lett.* **112**, 241101 (2014), 1403.3985.
- [4] R. Flauger, J. C. Hill, and D. N. Spergel, *JCAP* **1408**, 039 (2014), 1405.7351.
- [5] M. J. Mortonson and U. Seljak (2014), 1405.5857.
- [6] A. H. Guth, *Phys.Rev.* **D23**, 347 (1981).
- [7] A. D. Linde, *Phys.Lett.* **B108**, 389 (1982).
- [8] A. Albrecht and P. J. Steinhardt, *Phys.Rev.Lett.* **48**, 1220 (1982).
- [9] D. Kazanas, *Astrophys.J.* **241**, L59 (1980).
- [10] A. A. Starobinsky, *Phys.Lett.* **B91**, 99 (1980).
- [11] K. Sato, *Phys.Lett.* **B99**, 66 (1981).
- [12] K. Sato, *Mon.Not.Roy.Astron.Soc.* **195**, 467 (1981).
- [13] V. F. Mukhanov and G. V. Chibisov, *JETP Lett.* **33**, 532 (1981).
- [14] V. F. Mukhanov (2003), astro-ph/0303077.
- [15] A. D. Linde, *Phys.Lett.* **B129**, 177 (1983).
- [16] M. S. Turner, *Phys.Rev.* **D55**, 435 (1997), astro-ph/9607066.
- [17] C. Ungarelli, P. Corasaniti, R. Mercer, and A. Vecchio, *Class.Quant.Grav.* **22**, S955 (2005), astro-ph/0504294.
- [18] A. Cooray, *Mod.Phys.Lett.* **A20**, 2503 (2005), astro-ph/0503118.
- [19] T. L. Smith, M. Kamionkowski, and A. Cooray, *Phys.Rev.* **D73**, 023504 (2006), astro-ph/0506422.
- [20] T. L. Smith, H. V. Peiris, and A. Cooray, *Phys.Rev.* **D73**, 123503 (2006), astro-ph/0602137.
- [21] S. Chongchitnan and G. Efstathiou, *Phys.Rev.* **D73**, 083511 (2006), astro-ph/0602594.
- [22] B. C. Friedman, A. Cooray, and A. Melchiorri, *Phys.Rev.* **D74**, 123509 (2006), astro-ph/0610220.
- [23] S. Kuroyanagi, S. Tsujikawa, T. Chiba, and N. Sugiyama (2014), 1406.1369.
- [24] R. Jinno, T. Moroi, and T. Takahashi (2014), 1406.1666.
- [25] L. Boyle, K. M. Smith, C. Dvorkin, and N. Turok (2014), 1408.3129.
- [26] J. Caligiuri and A. Kosowsky, *Phys.Rev.Lett.* **112**, 191302 (2014), 1403.5324.
- [27] W. H. Kinney, *Phys.Rev.* **D66**, 083508 (2002), astro-ph/0206032.
- [28] R. Easther and W. H. Kinney, *Phys.Rev.* **D67**, 043511 (2003), astro-ph/0210345.
- [29] C. R. Contaldi (2014), 1407.6682.
- [30] J. E. Lidsey, A. R. Liddle, E. W. Kolb, E. J. Copeland, T. Barreiro, et al., *Rev.Mod.Phys.* **69**, 373 (1997), astro-ph/9508078.
- [31] M. B. Hoffman and M. S. Turner, *Phys.Rev.* **D64**, 023506 (2001), astro-ph/0006321.
- [32] E. D. Stewart and D. H. Lyth, *Phys.Lett.* **B302**, 171 (1993), gr-qc/9302019.
- [33] D. Spergel et al. (WMAP Collaboration), *Astrophys.J.Suppl.* **148**, 175 (2003), astro-ph/0302209.
- [34] P. Ade et al. (Planck Collaboration), *Astron.Astrophys.* (2014), 1303.5076.
- [35] C. Bennett et al. (WMAP), *Astrophys.J.Suppl.* **208**, 20 (2013), 1212.5225.
- [36] C. P. Ahn et al. (SDSS Collaboration), *Astrophys.J.Suppl.* **203**, 21 (2012), 1207.7137.
- [37] D. H. Jones, M. A. Read, W. Saunders, M. Colless, T. Jarrett, et al. (2009), 0903.5451.
- [38] C. Blake, E. Kazin, F. Beutler, T. Davis, D. Parkinson, et al., *Mon.Not.Roy.Astron.Soc.* **418**, 1707 (2011), 1108.2635.
- [39] K. Freese and W. H. Kinney (2014), 1403.5277.
- [40] T. L. Smith, M. Kamionkowski, and A. Cooray, *Phys.Rev.* **D78**, 083525 (2008), 0802.1530.
- [41] Y. Watanabe and E. Komatsu, *Phys.Rev.* **D73**, 123515 (2006), astro-ph/0604176.
- [42] S. Weinberg, *Phys.Rev.* **D69**, 023503 (2004), astro-ph/0306304.
- [43] S. Kawamura, T. Nakamura, M. Ando, N. Seto, K. Tsubono, et al., *Class.Quant.Grav.* **23**, S125 (2006).
- [44] L. Knox and Y.-S. Song, *Phys.Rev.Lett.* **89**, 011303 (2002), astro-ph/0202286.
- [45] C. M. Hirata and U. Seljak, *Phys.Rev.* **D68**, 083002 (2003), astro-ph/0306354.
- [46] A. Kogut, D. Fixsen, D. Chuss, J. Dotson, E. Dwek, et al., *JCAP* **1107**, 025 (2011), 1105.2044.
- [47] S. Kuroyanagi, T. Chiba, and N. Sugiyama, *Phys.Rev.* **D83**, 043514 (2011), 1010.5246.
- [48] L. Dai, M. Kamionkowski, and J. Wang, *Phys.Rev.Lett.* **113**, 041302 (2014), 1404.6704.
- [49] S. Dodelson, *Phys.Rev.Lett.* **112**, 191301 (2014), 1403.6310.